Institute of Experimental Morphology, Pathology and Anthropology with Museum
Bulgarian Anatomical Society

Acta morphologica et anthropologica, 27 (1-2)
Sofia ● 2020

ANTHROPOLOGY AND ANATOMY 27 (2)

Original Articles

Digital Morphometric Analysis and Comparison of Orbital Region in Metopic and Non-metopic Cranial Series

Silviya Nikolova[1], Diana Toneva[1], Angel Dandov[2]*

[1]Department of Anthropology and Anatomy, Institute of Experimental Morphology, Pathology and Anthropology with Museum, Bulgarian Academy of Sciences, Sofia, Bulgaria
[2]Department of Anatomy and Histology, Medical University, Sofia, Bulgaria

* Corresponding author e-mail: sil_nikolova@abv.bg

The study aimed to compare the orbital region in metopic and non-metopic series and to ascertain if its morphology differs considerably in both of them. A total of 278 (control, n = 207; metopic series, n = 71) dry skulls of contemporary adult males were scanned with a hand-held laser scanner. Digital morphometry was performed by recording the 3D coordinates of five bilateral landmarks. The linear measurements were calculated as Euclidian distances between the landmarks. Orbital index and orbital aperture area were also computed. The results showed that the metopic skulls had significantly larger upper biorbital (fmo-fmo), biorbital (ek-ek) and maxillofrontal (mf-mf) breadths. The orbital aperture area, orbital index and its distribution by categories did not differ considerably between the series. Generally, the metopic suture persistence was related to aspecific orbital region morphology. The established greater biorbital breadths in the metopic series were due to the enlarged intraorbital distance.

Key words: metopic suture, metopism, orbital region, polygonal 3D models, digital morphometry

Introduction

The frontal bone undergoes intramembranous ossification during embryogenesis and develops from two ossification centres. The metopic suture forms at the borderline between both halves of the growing frontal bone and runs from the *nasion* to the anterior fontanelle. The metopic suture allows enlargement of the frontal part of neurocranoium

perpendicular to it. This suture is the first one which physiologically obliterates, usually by the end of the second postnatal year. The fusion is initiated at the *nasion* and progresses towards the anterior fontanelle [3]. Sometimes, however, the closure is delayed and the metopic suture persists during the adulthood. In such cases, the frontal bone remains bipartite and this condition is known as *metopism*. The hypothetical factors causing *metopism* are with heterogeneous etiology and are still unclear. The reported frequency varies in wide ranges among the different groups [1, 8, 12, 15, 16].

It is known that the cranial sutures allow growth of the adjacent bone plates in direction perpendicular to the suture line. In accordance to this regularity, the metopic skulls have been observed to possess a considerably wider frontal bone [15, 16, 19]. The orbital region of the skull includes the two orbits, which are symmetrical bony cavities. Each orbit is shaped like a four-sided pyramid, with its apex situated posteriorly and its base anteriorly. The orbital aperture is enclosed by the frontal bone superiorly, the zygomatic bone laterally and the maxilla inferiorly. Since the frontal bone partakes in the orbit formation, it is reasonable to suppose that the orbital region in metopic skulls differs as well. Therefore, the aim of this study was to compare the orbital region in metopic and non-metopic cranial series using digital morphometric analysis. This way we intended to assess the relation of the metopic suture persistence to the orbital region morphology.

Materials and Methods

A total of 278 dry adult male skulls without mandibles were investigated. The skulls were distributed into two groups: a metopic series (n = 71) with a patent metopic suture extending from *nasion* to *bregma* and a control series (n = 207) without any traces of metopic suture. The skulls belonged to soldiers who died in the wars at the beginning of the 20th century. The bone remains were preserved at the Military Mausoleum with Ossuary and were kindly provided for investigation by the Bulgarian National Museum of Military History.

Generation of 3D polygonal models

The skulls were scanned with a hand-held laser scanner CreaformVIUscan. The scanning was performed at a resolution of 0.40 mm and a texture resolution of 150 DPI. The accuracy of the laser scanner was up to 0.05 mm. The collected surface data were post-processed in the scanner software platform VXelements™.

Digital morphometry

Digital morphometry was performed on the polygonal models (**Fig. 1**) by recording the 3D coordinates of five bilateral landmarks (**Table 1**) using the "Pick Points" tool in the free software MeshLab version2016.12 [2] (**Fig. 2**). The linear distances were calculated as Euclidian distances using the software PAST version 2.17c. [4]. The measurements obtained from 3D models generated by laser scanning have been proved to be accurate and reliable [20-22].

The orbital index was calculated and distributed by categories according to the following borderline values [5]:

Chamaeconch × – 75.9
Mesoconch 76.0 – 84.9
Hypsiconch 85.0 – ×

The orbital aperture area was also computed using the formula for rectangle area calculation as was suggested by Kadanoff and Mutafov [5]. Accordingly, the orbital area was calculated as follows:

Orbital aperture area = Orbital breadth × Orbital height

Statistics

Basic descriptive statistics, including the mean, standard deviation (SD), minimum and maximum values, were calculated for both metopic and control series. The significance of the differences between groups was assessed by the independent samples t-test. The Mann-Whitney U-test was used in cases when the normality test or the equal variance test failed. Chi-square test was used to assess the intergroup differences in the distribution of the orbital index categories. The significance level for all tests was set at $p \leq 0.05$.

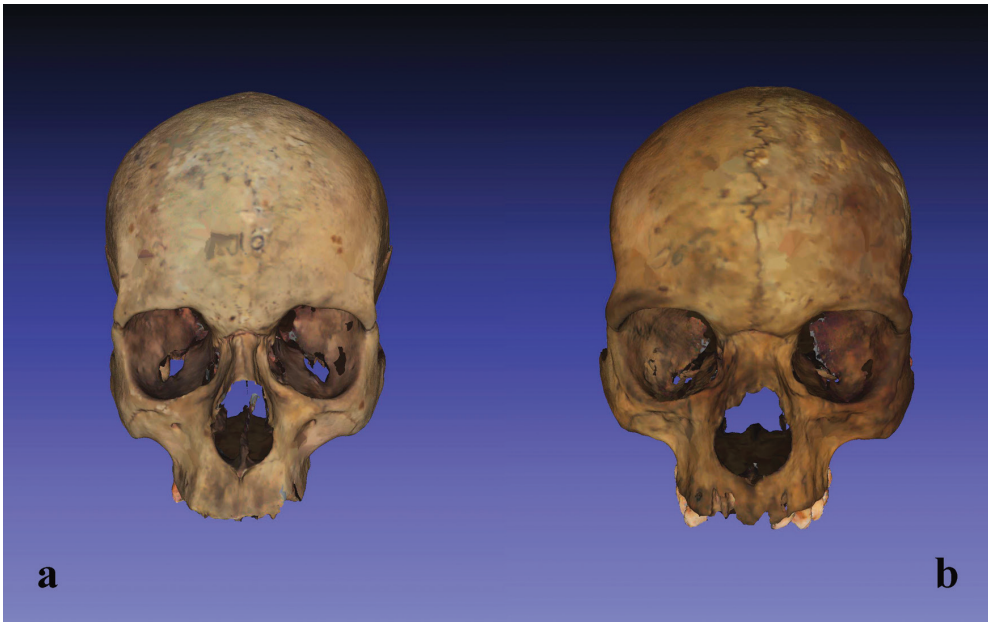

Fig. 1. Polygonal 3D models of skulls generated by laser scanning: a) a skull from the control series; b) a skull from the metopic series.

Table 1. Description of the landmarks and measurements

Landmarks	**Description**
Frontomalareorbitale (fmo)	The point of intersection of the zygomaticofrontal suture with the lateral orbital rim;
Ektoconchion (ek)	The point where the outer orbital rim length line, parallel to the upper border, meets the outer rim;
Maxillofrontale (mf)	The point of intersection of the anterior lacrimal crest with the frontomaxillary suture;
Supraorbitale (so)	The most superior point at the upper orbital rim;
Zygoorbitale (zo)	The point of intersection of the zygomaticomaxillary suture with the lower orbital rim;

Measurements	Description
Upper biorbital breadth (fmo-fmo)	The linear distance between both landmarks frontomalareorbitale;
Biorbital breadth (ek-ek)	The linear distance between both landmarks ektoconchion;
Orbital breadth R/L (mf-ek)	The linear distance between the landmarks maxillofrontale and ektoconchion;
Orbital height R/L (so-zo)	The linear distance between the landmarks supraorbitale andzygoorbitale;
Maxillofrontal breadth (mf-mf)	The linear distance between both landmarks maxillofrontale;
Indices	**Description**
Orbital index R/L (so-zo/mf-ek)	The ratio between the orbital height and the orbital length;
Area	**Description**
Orbital aperture area R/L	The multiplication of orbital width with orbital height.

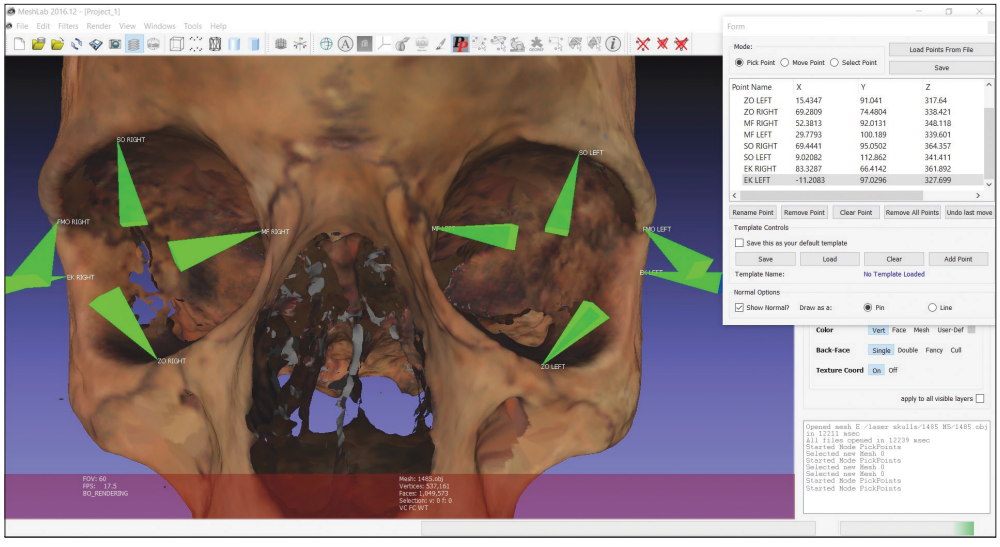

Fig. 2. Designation of the landmarks picked on a 3D model in MeshLab. Abbreviations: FMO – frontomalareorbitale; EK – ektoconchion; MF – maxillofrontale; SO – supraorbitale; ZO – zygoorbitale.

Results

Statistically significant differences between both series were observed in the upper biorbital breadth (fmo-fmo), biorbital breadth (ek-ek) and maxillofrontal breadth (mf-mf), which were larger in the metopic series. Besides, the orbital breadth (mf-ek) on the right side was significantly larger in the control series (**Table 2**). The orbital aperture area along with the orbital index and its distribution by categories did not differ significantly between the series (**Table 2, Table 3; Table 4**).

Table 2. Descriptive and test statistics of the measurements. The linear measurements are in mm and the area is in mm^2

Measurements	Metopic series					Control series					t-test/U-test (p-value)
	n	mean	SD	min	max	n	mean	SD	min	max	
Upper biorbital breadth (fmo-fmo)	70	98.97	3.03	93.02	106.66	207	97.35	3.64	88.12	109.04	t = 3.344 (P = <0.001)
Biorbital breadth (ek-ek)	70	97.86	2.64	91.83	104.06	206	96.69	3.52	88.90	108.21	U = 5670.50 (P = 0.008)
Orbital breadth R (mf-ek)	70	41.09	1.84	37.43	45.29	206	41.67	1.92	37.02	46.48	t = -2.192 (P = 0.029)
Orbital breadth L (mf-ek)	72	41.17	1.64	37.37	44.68	206	41.33	1.87	36.56	46.52	t = -0.649 (P = 0.517)
Orbital height R (so-zo)	70	33.48	2.33	27.13	38.90	207	33.56	2.10	27.49	39.52	t = -0.247 (P = 0.805)
Orbital height L (so-zo)	71	33.51	2.28	26.32	38.27	207	33.66	2.02	27.74	39.71	t = -0.547 (P = 0.585)
Maxillofrontal breadth (mf-mf)	71	22.57	2.12	18.13	28.78	206	19.95	2.06	15.04	26.63	t = 9.190 (P = <0.001)
Orbital index R (so-zo R/mf-ek R)	70	81.55	5.61	68.80	94.58	206	80.70	5.21	65.29	97.41	t = 1.157 (P = 0.248)
Orbital index L (so-zo L/mf-ek L)	71	81.45	5.72	63.71	93.02	207	81.54	4.98	64.94	95.32	t = -0.124 (P = 0.902)
Orbital area R (so-zo R*mf-ek R)	70	1377.33	130.39	1084.33	1641.17	207	1400.65	122.83	1088.22	1747.11	t = -1.351 (P = 0.178)
Orbital area L (so-zoL*mf-ekL)	71	1380.63	119.17	1087.56	1620.46	206	1392.87	122.37	1075.26	1847.24	t = -0.731 (P = 0.465)

Table 3. Distribution by orbital index categories

Orbital index categories	Metopic series R		Metopic series L		Control R		Control L	
	n	%	n	%	n	%	n	%
Chamaeconch	14	20.00	12	16.90	37	17.96	26	12.62
Mesoconch	37	52.86	41	57.75	125	60.68	124	60.19
Hypsiconch	19	27.14	18	25.35	44	21.36	56	27.18
Total	**70**	**100**	**71**	**100**	**206**	**100**	**206**	**100**

Table 4. Comparison between the distributions of orbital index categories in metopic and control series

Comparisons	χ^2(k = 2)	***p* value**
MS (R) : Control (R)	1.4279	0.489718
MS (L) : Control (L)	0.8246	0.662142

Discussion

The persistence of the metopic suture in adults has not been reported to cause any abnormalities by itself, though it has been found as a concomitant finding in some disorders [9, 11]. Furthermore, the metopic skulls often manifest additional bones, arising from non-fusion of normal ossification centres or from additional ones [9, 10, 13, 19]. It has also been observed that the metopic skulls possess a specific distinctive configuration of the neurocranium [15, 16, 19]. However, despite the close developmental interrelation between the neuro- and basicranium, the persisting metopic suture has not been associated with an alteration in the cranial base assessed by the cranial base angle constructed between the landmarks *nasion*, *sella* and *basion* [14]. The main differences concern the frontal bone, which is considerably shorter, wider and more convex in the metopic skulls [15, 19]. The significantly broad and high forehead in the metopic series, however, is not related to a greater frontal sinus pneumatization. On the contrary, recent morphometric investigations have revealed a tendency for metopic suture persistence to be frequently related to frontal sinus underdevelopment. Furthermore, the frontal sinus pneumatization seems to be a spatially-coordinated process progressing proportionately in the vertical and horizontal plates of the frontal bone [12, 15-18].

According to the functional matrix concept of Moss [6, 7] the adult human frontal bone is a single morphological structure, but not a single functional unit. The shape of the frontal bone accurately reflects the functional demands to protect and support the soft tissues and cavities. Thus, the metopic suture persistence could be considered not as a causative for the distinctive skull configuration, but rather as an expression of the underlying neural mass specific demands. The results obtained in this study show that besides the specific configuration on the frontal bone, the orbital region morphology in metopic skulls differs as well. As it could be seen, the orbital

aperture area and measurements do not differ considerably between the series, and the greater biorbital breadths in the metopic series are due to the significantly enlarged intraorbital distance, which in turn is a precondition for a broad nasal bridge. The tendency for a wider frontal bone and orbital region in metopic skulls is apparent, but the issue if the metopic suture retention causes this specific appearance, or all these features are the expression of underlying neural mass demands is still unclear and an object of further investigations.

Conclusion

It could be concluded that the persistence of a metopic suture is related to a distinct morphology of the orbital region, which is significantly wider in the metopic skulls. The greater biorbital breadths are not at the expense of enlarged orbital apertures, but are due to a greater interorbital distance.

Acknowledgements: The study was supported by the Bulgarian National Science Fund, Grants No DN01/15-20.12.2016 and DN11/9-15.12.2017. The authors thank Dr. Ivan Georgiev for the image generation.

References

1. **Berry, A. C.** Factors affecting the incidence of non-metrical skeletal variants. – *J. Anat.*, **120**, 1975, 519-535.
2. **Cignoni, P., M. Callieri, M. Corsini, M. Dellepiane, F. Ganovelli, G. Ranzuglia.** MeshLab: an open-source mesh processing tool. – *In: Eurographics*, *Italian Chapter Conference* (Eds. V. Scarano, R. De Chiara, U. Erra). Eurographics Association, 2008, 1-8.
3. **Faro, C., B. Benoit, P. Wegrzyn, R. Chaoui, K. Nicolaides.** Three-dimensional sonographic description of the fetal frontal bones and metopic suture. – *Ultrasound in Obstetrics & Gynecology*, **26**, 2005, 618-621.
4. **Hammer, Ø., D. Harper, P. Ryan.** PAST: paleontological statistics software package for education and data analysis. – *Palaeontologia Electronica*, **4**, 2001, 9-18.
5. **Kadanoff, D., S. Mutafov.** *The human skull in a medico-anthropological aspect: form, dimensions and variability*. Sofia, Prof. Marin Drinov Academic Publishing House. 1984, 236 pp
6. **Moss, M. L.** Functional anatomy of cranial synostosis. – *Childs Brain*., **1**, 1975, 22-33.
7. **Moss, M. L., R. W. Young.**A functional approach to craniology. – *Am. J. Phys. Anthropol.,* **18**, 1960, 281-292.
8. **Nikolova, S., D. Toneva.** Frequency of metopic suture in male and female medieval cranial series. – *Acta Morphol. Anthropol*., **19**, 2012, 250–252.
9. **Nikolova, S., D.Toneva, Y. Yordanov, N. Lazarov**. Multiple Wormian bones and their relation with definite pathological conditions in a case of an adult cranium. – *Anthropol. Anz.*, **71**, 2014, 169-190.
10. **Nikolova, S., D. Toneva, Y. Yordanov, N. Lazarov**. Variations in the squamous part of the occipital bone in medieval and contemporary cranial series from Bulgaria. – *Folia Morphol*., **73**, 2014, 429-438.
11. **Nikolova, S., D. Toneva, I. Georgiev.** A case of skeletal dysplasia in bone remains from a contemporary male individual. – *Acta Morphol. Anthropol*., **22**, 2015, 97-107.
12. **Nikolova, S., D. Toneva, I. Georgiev**. A persistent metopic suture – incidence and influence on the frontal sinus development (preliminary data). – *Acta Morphol. Anthropol*., **23**, 2016, 83-90.
13. **Nikolova, S., D. Toneva, I. Georgiev, Y. Yordanov, N. Lazarov**. Two cases of large bregmatic bone along with a persistent metopic suture from necropoles on the northern Black Sea coast of Bulgaria. – *Anthropological Science*, **124**, 2016, 145-153.
14. **Nikolova, S., D. Toneva, I. Georgiev**. Cranial base angulation in metopic and non-metopic cranial series. – *Acta Morphol. Anthropol.,* **24**, 2017, 45-49.

15. **Nikolova, S., D. Toneva, I. Georgiev, N. Lazarov**. Digital radiomorphometric analysis of the frontal sinus and assessment of the relation between persistent metopic suture and frontal sinus development. – *Am. J. Phys. Anthropol*., **165**, 2018, 492-506.
16. **Nikolova, S., D. Toneva, I. Georgiev,N. Lazarov**. Relation between metopic suture persistence and frontal sinus development. – In: *Challenging issues on paranasal sinuses* (Ed. Tang-Chuan Wang), IntechOpen, 2018, 3-23.
17. **Nikolova, S., D. Toneva, I. Georgiev, A. Dandov, N. Lazarov**. Morphometric analysis of the frontal sinus: application of industrial digital radiography and virtual endocast. – *JOFRI*, **12**, 2018, 31-39.
18. **Nikolova, S., D. Toneva.** Frontal sinus dimensions in the presence of persistent metopic suture**.** – *Acta Morphol. Anthropol*., **26**, 2019, 92-98.
19. **Nikolova, S., D. Toneva, G. Agre, N. Lazarov**. Data mining for peculiarities in the configuration of neurocranium when the metopic suture persists. – *Anthropol. Anz.,* 2019 (*in press*) DOI: 10.1127/anthranz/2019/1051
20. **Toneva, D., S. Nikolova, I. Georgiev.** Reliability and accuracy of angular measurements on laser scanning created 3D models of dry skulls. **–** *J. Anthropol.*, **2016**, 2016, 1-6.
21. **Toneva, D., S. Nikolova, I. Georgiev, A. Tchorbadjieff.** Accuracy of linear craniometric measurements obtained from laser scanning created 3D models of dry skulls. – In: *Advanced computing in industrial mathematics. Studies in computational intelligence* (Eds. Georgiev, K., M. Todorov, I. Georgiev), **681**, Springer, 2017, 215-229.
22. **Toneva, D., S. Nikolova, I. Georgiev, N. Lazarov**. Impact of resolution and texture of laser scanning generated 3D models on landmark identification. – *Anat. Rec.* (Hoboken), 2019 (*in press)* DOI: 10.1002/ar.24272